Early Stages of Misfolding and Association of β_2-Microglobulin: Insights from Infrared Spectroscopy and Dynamic Light Scattering[†]

Heinz Fabian,*[,‡] Klaus Gast,*[,§] Michael Laue,[||] Rolf Misselwitz,[⊥] Barbara Uchanska-Ziegler,[⊥] Andreas Ziegler,[⊥] and Dieter Naumann[‡]

Robert Koch-Institut, P 25 and ZBS4, Nordufer 20, D-13353 Berlin, Germany, Institut für Physikalische Biochemie, Universität Potsdam, Karl-Liebknecht-Strasse 24-25, D-14476 Golm/Potsdam, Germany, and Institut für Immungenetik, Charité-Universitätsmedizin Berlin, Freie-Universität Berlin, Thielallee 73, D-14195 Berlin, Germany

Received February 18, 2008; Revised Manuscript Received May 7, 2008

ABSTRACT: Conformational changes associated with the assembly of recombinant β_2-microglobulin *in vitro* under acidic conditions were investigated using infrared spectroscopy and static and dynamic light scattering. In parallel, the morphology of the different aggregated species obtained under defined conditions was characterized by electron microscopy. The initial salt-induced aggregate form of β_2-microglobulin, composed of small oligomers (dimers to tetramers), revealed the presence of β-strands organized in an intramolecular-like fashion. Further particle growth was accompanied by the formation of intermolecular β-sheet structure and led to short curved forms. An increase in temperature by only 25 °C was able to disaggregate these assemblies, followed by the formation of longer filamentous structures. In contrast, a rise in temperature up to 100 °C was associated with a reorganization of the short curved forms at the level of secondary structure and the state of assembly, leading to a species with a characteristic infrared spectrum different from those of all the other aggregates observed before, suggesting a unique overall structure. The infrared spectral features of this species were nearly identical to those of β_2-microglobulin assemblies formed at low ionic strength with agitation, indicating the presence of fibrils, which was confirmed by electron microscopy. The observed spectroscopic changes suggest that the heat-triggered conversion of the short curved assemblies into fibrils involves a reorganization of the β-strands from an antiparallel arrangement to a parallel arrangement, with the latter being characteristic of amyloid fibrils of β_2-microglobulin.

β_2-Microglobulin (β_2m)[1] is a 99-residue protein that represents the noncovalently bound nonpolymorphic light chain of major histocompatibility complex class I molecules (*1*). Native β_2m exhibits a seven-stranded β-sandwich structure organized into two β-sheets connected by a single disulfide bond linking Cys25 and Cys80 (*2*). β_2m is also the major component of the amyloid deposits that are found in the musculoskeletal system in patients suffering from dialysis-related amyloidosis (*3–5*). Although one of the most extensively studied amyloidogenic proteins, the mechanisms by which soluble β_2m is converted into β_2m amyloid fibrils *in vivo* are still largely unknown. *In vitro*, β_2m has been shown to be stably folded at physiological pH and intransigent to assembly into amyloid fibrils, and it is assumed that partial unfolding of the native protein is required for fibrillation to be initiated. Several groups have studied the formation of fibrils at neutral pH by incubation of the full-length protein in the presence of copper ions (*6, 7*), by truncation of six amino acids from the N-terminus (*8*), by addition of organic solvents (*9*) or sodium dodecyl sulfate (*10*), by ultrasonication (*11*), by addition of preformed β_2m seeds (*12*), or in the presence of collagen (*13*). Amyloid-like fibrillar structures of wild-type β_2m can form more easily and with high yield under acidic conditions, when the protein is initially partially or fully unfolded, both by extension of *ex vivo* material (*14, 15*) or in a self-nucleated manner (*16, 17*).

Depending on the growth conditions used, fibrillar structures of different morphologies are formed. For example, straight needle-like amyloid fibrils can be formed *in vitro* by the seed-dependent extension reaction at pH 2.5, in which seeded fibrils are added to monomeric β_2m (*14*). With agitation, long straight fibrils of similar shape can form spontaneously with a lag phase at pH 2.5 and low ionic strength also in the absence of seeds (*17, 18*). Incubation of β_2m at pH ~3.6 at high ionic strength results in the formation only of short curved worm-like structures that are trapped as end products of an assembly (*19, 20*). Without agitation, β_2m seems not to be fibrillogenic around pH 2.5 at low ionic strength (*21*) but can form elongated beaded structures, often referred to as protofibrils, in this pH range at ionic strengths of 0.2−0.4 M (*16, 19–22*). These salt-induced protofibrils can be converted by drastic heat treatment into mature fibrils,

[†] This work was supported by the Deutsche Forschungsgemeinschaft (Na 226/12-2, SFB 449 TP B6, Ga 530/2-2).

* Corresponding authors. H.F.: tel, 49-30-45472202; fax, 49-30-45472606; e-mail, fabianh@rki.de. K.G.: tel, 49-331-9775267; fax, 49-331-9775062; e-mail, khpgast@rz.unipotsdam.de.

[‡] Robert Koch-Institut, P 25.

[§] Universität Potsdam.

[||] Robert Koch-Institut, ZBS4.

[⊥] Freie-Universität Berlin.

[1] Abbreviations: β_2m, β_2-microglobulin; IR, infrared; SLS, static light scattering; DLS, dynamic light scattering; EM, electron microscopy; CD, circular dichroism.

10.1021/bi800279y CCC: $40.75
Published on Web 06/10/2008

as observed in a recent study (*23*). Although the amyloid fibrils formed under acidic conditions are not stable at physiological pH (*22, 24*), and their relevance *in vivo* is consequently unclear, these conditions are ideal for an analysis of the process of β_2m assembly under different kinetic regimes.

Here we describe a series of experiments using infrared (IR) spectroscopy and static (SLS) as well as dynamic light scattering (DLS) to directly correlate changes in secondary structure with variations in the state of association during the early stages of assembly of β_2m. Specifically, filamentous species formed after adding sodium chloride to the acid-unfolded state of β_2m are described, and their presence and kinetics of assembly are validated directly using the combined IR and SLS/DLS approach. Moreover, we studied the impact of moderate and extended heat treatment on the salt-induced assemblies of β_2m.

MATERIALS AND METHODS

Protein Expression and Purification. β_2m was overexpressed in *Escherichia coli* as inclusion bodies and purified to homogeneity as described previously (*25*). An N-terminal initiating Met residue (Met0) was incorporated into 95% of β_2m prepared by this method. The purified protein was extensively dialyzed against water and lyophilized. For the experiments at physiological pH, the lyophilized protein was dissolved in D_2O buffer (50 mM sodium cacodylate, pH 7.5). For the measurements at low pH, the samples were first dissolved in 10 mM deuterium chloride (DCl) and lyophilized again. Prior to the experiments, the samples were then dissolved in 2 mM DCl, yielding a sample pH of ~2.4 (electrode readings are uncorrected for deuterium isotope effects). The concentration of the protein samples was determined spectrophotometrically at 280 nm ($A^{1cm}{}_{1\%} = 16.17$) (*23*).

Laser Light Scattering. SLS and DLS data were measured simultaneously with one and the same instrument at a scattering angle of 90°. A laboratory-built apparatus, equipped with a diode-pumped, continuous wave laser Millenia IIs (Spectra Physics) and a high quantum yield avalanche photodiode, was employed. Details of the detection and data processing procedures, which were specifically developed for kinetic experiments, have been described elsewhere (*26*). Apparent molecular masses were estimated from the relative scattering intensities using toluene as a reference sample and applying a refractive index increment $(\partial n/\partial c) = 0.19$ mL/g. The translational diffusion coefficients D were obtained from the measured autocorrelation functions using either the program CONTIN (*27*) or applying the method of cumulants (*28*). The diffusion coefficients were converted into Stokes radii via the Stokes−Einstein equation $R_S = k_BT/(6\pi\eta_0 D)$, where k_B is Boltzmann's constant, T is the temperature in kelvin, and η_0 is the solvent viscosity. In order to remove dust and other large particles, the samples were centrifuged for 1 h at 75000g and transferred into precleaned 3 mm × 3 mm fluorescence cells (Hellma, Müllheim, Germany). For measurements of salt-induced changes, appropriate amounts of prefiltered stock solutions were mixed with salt-free protein within the scattering cells. Temperature jumps were achieved by inserting the scattering cells into the preheated sample holder.

Infrared Spectroscopy. The protein solutions were placed into demountable CaF_2 IR cells (*29*) with an optical path length of 50 μm. Infrared spectra were recorded with Bruker IFS-28B and Bruker IFS-66 Fourier transform infrared (FTIR) spectrometers that were continuously purged with dry air and equipped with deuterated triglycine sulfate (DTGS) detectors. For each sample, either 32 (at the beginning of the kinetic experiments) or 128 interferograms (at later time points) were coadded and Fourier transformed with a zero filling factor of 4 to yield spectra with a nominal resolution of 4 cm^{-1} (~1 data point per 1 cm^{-1}). The sample temperature was controlled by means of a thermostated cell jacket (*29*). In order to minimize problems due to baseline drifts of the spectrometer or variations of the dry atmosphere in the spectrometer, the sample in the cell jacket was mounted in a motor-driven sample shuttle, which allowed recording of the background immediately before recording of the sample spectrum without opening the sample chamber of the spectrometer. Solvent spectra were recorded under identical conditions and subtracted from the spectra of the proteins in the relevant D_2O solvent and at the relevant temperature. Spectral contributions from residual water vapor, if present, were eliminated using a set of water vapor spectra. The final unsmoothed protein spectra were used for further analysis. Band positions and band intensities were determined by standard modules of the Bruker OPUS software, which were implemented into home-built macros for data analysis. Second derivatives were obtained using the Savitzky−Golay algorithm with 13-point smoothing. Intensity/temperature plots of the IR data were created using the ORIGIN software.

Negative Staining Electron Microscopy. Sample suspensions were used at a concentration of about 0.1 mg/mL by dropping 10 μL of each suspension onto the plastic film (carbon-coated Formvar) of a sample support (copper grid, 3.05 mm in diameter, 400 mesh). The plastic film surface had been treated with 0.25% aqueous Bacitracin (10 min, room temperature) for a better adsorption of the particles. After 10 min of incubation, the plastic film surfaces were briefly washed on four succeeding droplets (30 μL each) of bidistilled water and contrasted by attaching the films briefly to a drop of 1% uranyl acetate. Finally, plastic films were blotted dry with a filter paper and inspected with a transmission electron microscope operated at 120 kV (Tecnai Spirit, FEI Co.). Images were recorded with a CCD camera (Megaview III; Olympus Soft Imaging Solutions) at a resolution of 1376 × 1032 pixels. The length of the assemblies was measured using a semiautomatic procedure and the ImageJ program (*30*). The assemblies were first labeled in black with a marker tool of a defined size before the gray-level image was converted into a binary image (i.e., black and white) using the threshold function for a segmentation of the labeled particles. The image was then analyzed automatically by the "Analyze particles" routine of the program, resulting in number and circumference of the segmented particles. Finally, the length of individual particles was calculated with the spreadsheet program MS Excel, and the distribution of all measurements was plotted as a histogram using the ORIGIN software.

Light Scattering Controls of Aggregation. Light scattering was also monitored with a Varian Cary Eclipse spectrofluorometer using a quartz cell with a light path of 3 mm. For

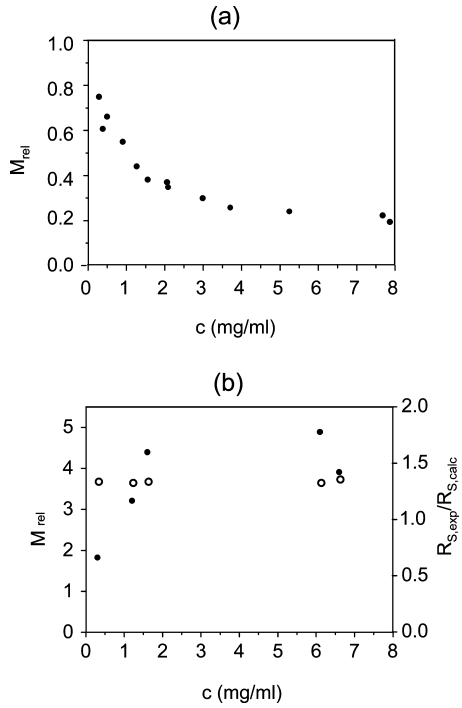

FIGURE 1: Concentration dependence of the relative molecular masses of (a) acid-unfolded β_2m in 2 mM DCl, pH 2.4, and (b) 2 min after addition of NaCl to acid-unfolded β_2m (final solvent conditions 0.2 M NaCl, pH 2.1). The open symbols in (b) represent the compactness of the salt-induced initial states of β_2m, given by the ratio $R_{s,exp}/R_{s,calc}$.

light scattering, the wavelengths for excitation and emission were both set at 500 nm. The temperature of the sample solutions was kept at the corresponding temperatures by a Peltier-controlled cell holder, equipped with a magnetic stirrer.

RESULTS

Characterization of the Initial Oligomerization State of β_2m. The molecular mass of β_2m at 25 °C in 2 mM DCL (pH ~2.4) was estimated in order to check whether the protein is a monomer under this condition. The true molecular mass could be obtained from integrated light scattering data by extrapolating the reciprocal values of the apparent mass, M_{app}, measured at a series of concentrations to zero concentration. However, the corresponding plot was highly nonlinear, preventing any proper extrapolation. The positive slope was indicative of strong repulsive intermolecular interactions in the absence of salt. Thus, it is more instructive to show the ratio $M_{rel} = M_{app}/M_{aa}$ in dependence of protein concentration (Figure 1a), where M_{aa} is the molecular mass calculated from the amino acid composition (11.86 kDa). M_{rel} was close to 1 at low concentration, indicating a monomeric acid-denatured state of β_2m (note: $M_{rel} < 1$ is observed at finite concentrations since M_{app} decreases with increasing concentration due to strong repulsive intermolecular interactions). M_{rel} will be used throughout this study as a measure of the state of aggregation of the protein. The analysis of the DLS data revealed also a nonlinear increase of the measured diffusion coefficient with increasing β_2m concentration (data not shown). Extrapolation to zero protein concentration suggested a diffusion coefficient of 9×10^{-7} cm^2/s, which corresponds to a Stokes radius of 2.3 nm. A translational diffusion coefficient $D = 12.4 \times 10^{-7}$ cm^2/s and a Stokes radius $R_s = 1.73$ nm were obtained for natively folded β_2m at neutral pH ($M_{app} = 11294$ g/mol, protein concentration 1.31 mg/mL).

The association of the β_2m molecules was induced by adding a stock solution of 1 M NaCl in 10 mM DCl to the acid-denatured samples. The final concentration of NaCl was 0.2 M (pH ~2.1). An increase in light scattering intensity was observed immediately after adding salt at all three β_2m concentrations. The absence of any lag phase indicated that nucleation seems not to be involved in the aggregation process under these experimental conditions. The first apparent molecular masses could be measured ~2 min after initiation of the aggregation process. The concentration dependence of the relative mass obtained 2 min after addition of NaCl (Figure 1b, solid symbols) was quite different from that of the salt-free monomer (Figure 1a), which reflects differences in the actual state of aggregation. In the case of the lowest concentration (0.3 mg/mL), the relative mass was still between those of monomer and dimer, while it was close to that of a tetramer at the higher protein concentrations.

Moreover, we compared the compactness of the initial structures of the β_2m molecules formed after addition of salt with those of the native protein molecule. This was achieved according to an established relation, the scaling law $R_S = aM^b$ between Stokes radius (in nm) and apparent molecular mass (in Da), with $a = 0.0557$ and $b = 0.369$ suggested by Uversky (*31*). A ratio $R_{S,exp}/R_{S,calc}$ between 1.33 and 1.36 was found for the salt-induced initial state (Figure 1b, open symbols), clearly different from the corresponding value of β_2m at neutral pH ($R_{S,exp}/R_{S,calc} = 0.99$; data not shown). This indicated that the initial state of β_2m aggregation at pH 2.1 was considerably less compact than those of natively folded β_2m. The data for the latter were in excellent agreement with the scaling law obtained for a number of other proteins (*31*).

IR spectroscopy, known to be a sensitive method to indicate the presence of and to monitor changes in β-sheet structures, was then employed to characterize secondary structural features of β_2m and to probe the kinetics of its assembly. To better visualize weak bands, the second derivatives of the IR spectra were calculated, which give a negative peak for every band or shoulder in the spectrum. The IR spectrum of native β_2m in D_2O buffer at pH 7.5 after complete H/D exchange (Figure 2a) exhibited a major amide I band component at 1633 cm^{-1} and a weaker band component at 1682 cm^{-1}, both together indicating the presence of intramolecular antiparallel β-sheet structures (*15*). A weak feature at 1670 cm^{-1} could be assigned to turn-like structures, while the IR bands between 1480 and 1600 cm^{-1} in fully H/D exchanged proteins are due to amino acid side chain absorptions (*32*). On the other hand, the well-separated tyrosine band at ~1515 cm^{-1} is a useful internal standard to normalize the IR spectra of a protein measured under different conditions since intensity changes of this band are minimal (*33*).

The IR spectrum of the acid-denatured protein in 2 mM DCl (Figure 2b, solid line) exhibited only a broad, nearly featureless amide I band contour centered at ~1639 cm^{-1}, typical of a fully or predominantly unordered protein structure. The addition of NaCl to the acid-unfolded protein induced the formation of secondary structure, as indicated by the weak features at 1632 and 1683 cm^{-1} in the spectrum

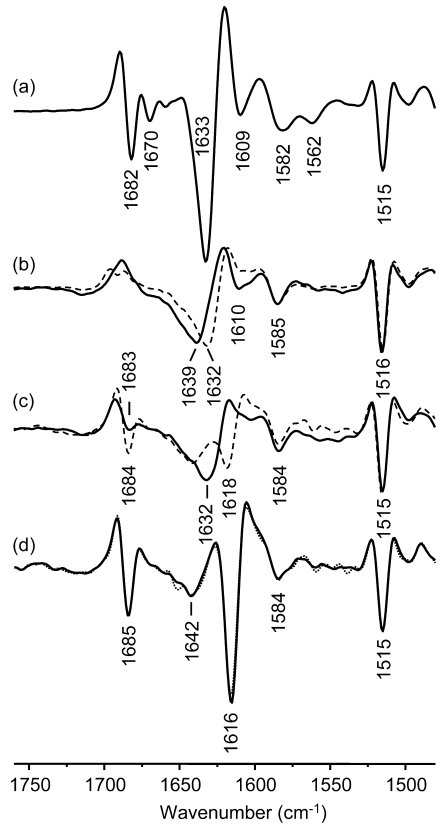

FIGURE 2: Infrared spectra (second derivatives) of different forms of β_2m. (a) Native protein in D_2O buffer (pH 7.5) after complete H/D exchange. Exchange of all amide protons with deuterons was achieved by keeping the protein solutions overnight at 37 °C and was verified by absence of the amide A band (N−H stretching vibration of the peptide groups) at ~3300 cm^{-1}. (b) Acid-unfolded β_2m in 2 mM DCl, pH 2.4 (solid line), and β_2m in 1 mM DCl, pH 3.4 (dashed line). (c) β_2m 3 min after addition of NaCl (solid line) and after 1 h (dashed line) (final protein concentration 1.2 mg/mL, solvent conditions 0.2 M NaCl, pH 2.1). (d) β_2m in the presence of 0.2 M NaCl after 40 h (dotted line) and 70 h (solid line). All spectra are drawn to the same scale based on the intensity of the tyrosine band at 1515 cm^{-1} as internal standard.

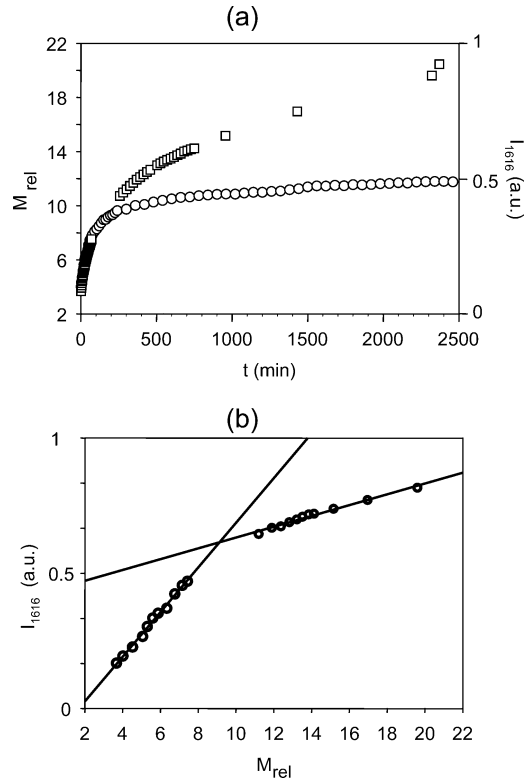

FIGURE 3: Association-induced structural changes of β_2m (1.2 mg/mL) in the presence of 0.2 M NaCl at 25 °C, pH 2.1. Formation of "A-type" assemblies. (a) Long-time kinetics probed by comparison of the changes in intensity of the IR band at 1616 cm^{-1} (circles), which directly monitors the formation of intermolecular β-sheet structure, with the changes in the relative mass of the aggregates (squares) as determined from the DLS data. (b) Temporal changes of the IR band at 1616 cm^{-1} (I_{1616}) versus changes of the relative molecular mass (M_{rel}), observed over a time period of 40 h.

(Figure 2c, solid line), but the positions of these two weak features were very similar to those of the strong amide I band components in the spectrum of the native protein (Figure 2a). Moreover, the frequencies and intensities of these β-sheet bands practically coincided with those observed at pH 3.4 in the absence of NaCl (Figure 2b, dashed line), conditions under which β_2m is known be to be partially denatured (*16*). Altogether, the IR data indicated the presence of β-strands organized in an intramolecular-like fashion in the initial salt-induced state of β_2m, which later disappeared as a function of time.

Subsequent Structural Changes during Aggregation of β_2m. One hour after initiation of the association process, a new band component at ~1618 cm^{-1} could be clearly observed (Figure 2c, dashed line), whose intensity increased over time. The strong low-frequency band component at ~1618 cm^{-1} and a weaker band component at ~1684 cm^{-1} indicated the presence of antiparallel intermolecular β-sheet structure in the aggregates. Almost identical IR spectra were obtained at 40 or 70 h after initiation of the event (compare the solid and dotted lines in Figure 2d), suggesting that under the experimental conditions employed, the formation of intermolecular β-sheet structure was practically completed after ~2 days. The broad feature centered at ~1642 cm^{-1} was consistent with the presence of residual disordered structures.

DLS and IR experiments carried out over 2 days under the same conditions (1.2 mg/mL, 0.2 M NaCl, pH 2.1, in DCl) revealed that the kinetics of intermolecular β-sheet formation for β_2m is complex and differed notably from the kinetics of aggregation of the protein after ~2 h (compare the circles and squares in Figure 3a). In order to relate the conversion in secondary structure to the state of oligomerization, it is useful to plot the temporal changes of the intensity of the IR band at 1616 cm^{-1} versus the changes of the relative apparent mass (Figure 3b). This plot clearly revealed two different phases of synchronous processes of structure conversion and association. A change in these processes was observed at the approximate stage of octamers. Since association is involved, the kinetic rate constants are expected to depend on protein concentration. Indeed, light scattering measurements at protein concentrations between 0.3 and 6.7 mg/mL revealed a significant concentration dependence of the initial rates of mass increase. These were plotted against the relative protein concentration in a double logarithmic scale, and a linear fit of the data yielded a slope of $m = 0.96$ (Figure S1 in the Supporting Information). This, in turn, pointed to a reaction order of 1.96, which is consistent with a second-order process.

To examine the morphology of the β_2m associates in samples kept for several days at room temperature, negative

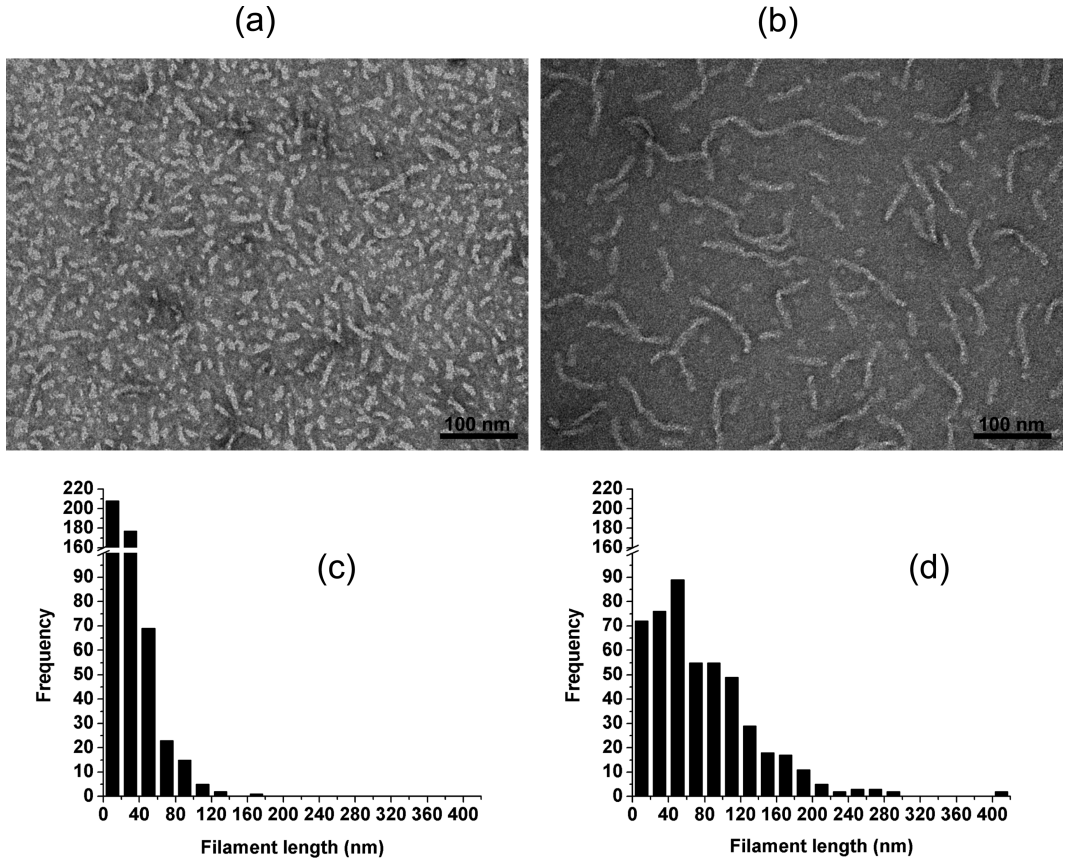

FIGURE 4: Electron micrographs of β_2m assemblies formed at pH 2.1 in the presence of 0.2 M NaCl. (a) After several days at ambient temperature ("A-type"). (b) After incubation for 20 h at 50 °C ("B-type"). The histograms in (c) and (d) show the respective filament length distribution of the "A-type" and "B-type" assemblies (approximately 500 samples each).

staining electron microscopy was performed. A typical image is shown in Figure 4a, indicating the presence of thin (~6 nm in width) and curved assemblies with an average length of ~40 nm (Figure 4c) (here termed "A-type" structures), in agreement with the results obtained previously by other groups under similar experimental conditions (*16, 17, 22*). No significant changes in morphology were observed even after months (data not shown), indicating that the observed structures, also called protofibrils (*22*), are stable structures under these conditions. Further experiments, however, revealed that moderate changes in the environmental conditions (e.g., an increase in temperature) may modify the features of these particular filamentous structures.

Heat-Triggered Disaggregation of the "A-Type" Particles of β_2m and Reassociation into a Different Species. Heat treatment of protein assemblies is known to trigger conformational alterations (*23*). In particular, a fast increase in temperature is effective in converting protofibrils of some proteins into amyloid fibrils (*34*). Therefore, we studied the impact of mild heat treatment on the salt-induced "A-type" assemblies of β_2m. For this purpose, the temperature of the corresponding β_2m samples in the IR or DLS cells was increased from 25 to 50 °C within 2−3 min, and conformational changes of the samples were monitored by the IR/SLS/DLS approach. The time course of the IR spectra of the β_2m sample exhibited initially a loss of band intensity at 1616 cm^{-1}, followed by a pronounced increase in intensity of this band as a function of incubation time at 50 °C. These characteristic spectral changes could best be resolved at lower protein concentrations, e.g., at 0.5 mg/mL, the lowest concentration feasible for collection of IR spectra (Figure 5a). The time course of the intensity of the IR "marker" band at 1616 cm^{-1} (Figure 6) indicated a loss of intermolecular β-sheet structure within the first 10−15 min, followed by a strong increase, which was not yet completed when the experiment was terminated after 18 h at 50 °C. This high amount of intermolecular β-sheet structure remained present also after cooling the sample to 25 °C and was much higher than that before the T-jump (compare the solid and dashed lines in Figure 5b).

SLS/DLS studies revealed corresponding characteristic changes in the relative molecular mass and Stokes radius as a function of incubation time at 50 °C (Figure 7a). There was a decrease in molecular mass observed within the first 5−10 min after the T-jump (Figure 7b), which indicated a disaggregation of the *salt-induced* "A-type" particles, followed by a reassembly into much larger structures. The degree of the disaggregation was remarkably dependent on protein concentration. This was mostly due to a concentration-independent rate of disaggregation and a strongly concentration-dependent rate of reassociation, which became evident by treating the data in the following manner: the time course of the changes in M_{rel} (Figure 7b) could be fitted by a phenomenological expression of the form

$$M_{rel} = M_{rel,min} + M_{rel,D} \exp(-k_D t) + s_{i,50} t \qquad (1)$$

Here, $M_{rel,min}$ is the minimum of the relative mass that is approached during disassembly/reassembly, $M_{rel,D}$ is the fraction of the relative mass by which M_{rel} is diminished

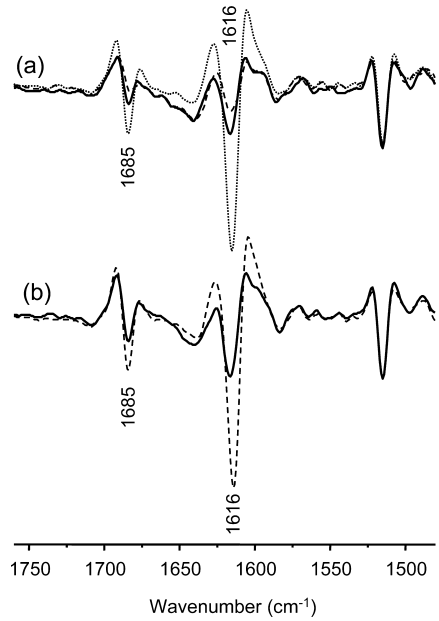

FIGURE 5: Characterization of the temperature-jump induced changes in secondary structure of the salt-induced "A-type" β_2m associates formed 1 day after addition of salt. Formation of "B-type" assemblies. (a) IR spectra (second derivatives) of β_2m (0.5 mg/mL, 0.2 M NaCl, pH 2.1) obtained at selected times after a T-jump from 25 to 50 °C: (solid line) after 2 min, (dashed line) after 15 min, (dotted line) after 18 h at 50 °C. (b) Comparison of the IR spectra obtained at 25 °C (solid line) before and (dashed line) after the T-jump.

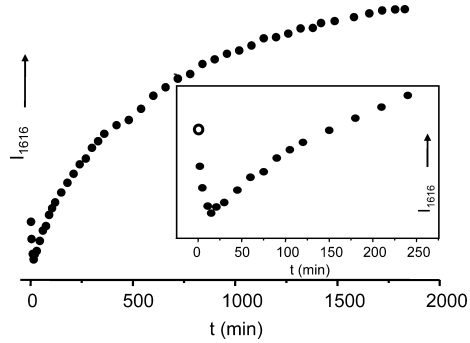

FIGURE 6: Partial unfolding of the "A-type" particles and subsequent re-formation of the intermolecular β-sheet structure of β_2m (0.5 mg/mL) in the presence of 0.2 M NaCl, pH 2.1, as depicted from absorbance changes of the IR band at 1616 cm^{-1} as a function of incubation time at 50 °C. The open circle (inset) shows the IR intensity at 1616 cm^{-1} at 25 °C before the T-jump.

during the exponential decrease with a rate constant k_D, and $s_{i,50}$ is the initial growth rate at 50 °C.

Practically identical disaggregation rates k_D of about 0.5 min^{-1} were obtained at the three different protein concentrations (Table 1). This verified the assumption of an exponential decay, as could be expected for a first-order process. By contrast, the initial growth rate at 50 °C revealed a pronounced and complicated dependence on protein concentration (Table 1). An interesting finding was that the minima of the average relative mass depended on protein concentration. This could not be explained solely by the relation between the decay rate k_D and the initial growth rate $s_{i,50}$. Since there was no indication of a faster initial growth rate, reassociation had to start at different oligomeric states. Only in the case of the lowest protein concentration studied in this work, the originally formed oligomers disassembled

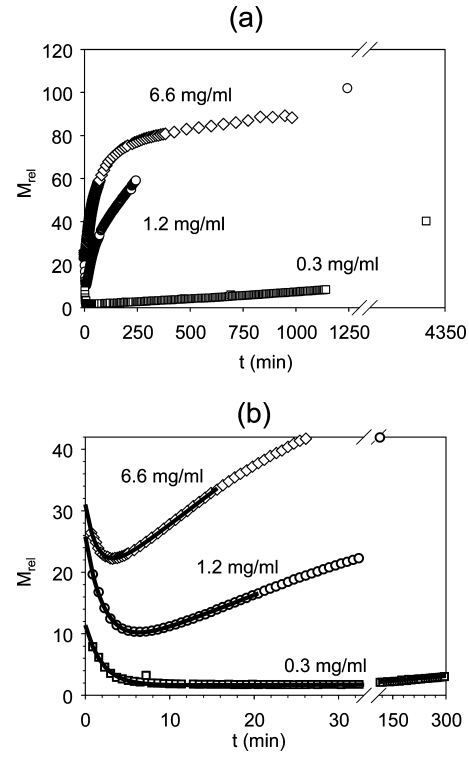

FIGURE 7: Concentration dependence of temperature-jump induced disaggregation of the "A-type" particles of β_2m in the presence of 0.2 M NaCl, pH 2.1, followed by reassembly to a new species ("B-type" particles), as depicted from the changes of the relative molecular masses as a function of incubation time at 50 °C (a) over 20 h. (b) Illustration of the initial temperature-induced disaggregation of the β_2m associates, which is almost complete at a protein concentration of 0.3 mg/mL. The solid lines represent the fits to the experimental data. The weak tendency of the β_2m molecules for reassociation permitted us to fit the data over 750 min in the case of the lowest protein concentration of 0.3 mg/mL.

almost completely to monomers ($M_{rel,min}$ ~1.6). Despite this strong dissociation and the weak reassociation rate at 0.3 mg/mL, an increase in relative molecular mass of up to 40 was observed after 3 days at 50 °C (Figure 7a). The larger values of $M_{rel,min}$ obtained at the higher concentrations (Table 1) suggested that not monomers but oligomers still present after minutes at 50 °C were the initial structures of the growing protofibrillar assemblies. These differences in the initial growth conditions may also have been the reason for the complicated concentration dependence, which could not be described throughout by a particular reaction order.

The combined IR and SLS/DLS studies on β_2m samples at a protein concentration of 1.2 mg/mL revealed practically identical kinetics for unfolding/re-formation of β-sheet structure on one side and disaggregation/reassociation of β_2m molecules on the other side (compare the open and solid circles in Figure 8a). In this case, a linear correlation between

Table 1: Kinetic Parameters of Disaggregation and Reassociation of β_2m after a T-Jump from 25 to 50 °C

	concn (mg/mL)		
	0.3	1.2	6.7
$M_{rel,min}$	1.59	5.65	17.3
$M_{rel,D}$	9.81	20.2	13.7
k_D (min^{-1})	0.50	0.443	0.660
$s_{i,50}$ (min^{-1})	0.0052	0.533	1.05

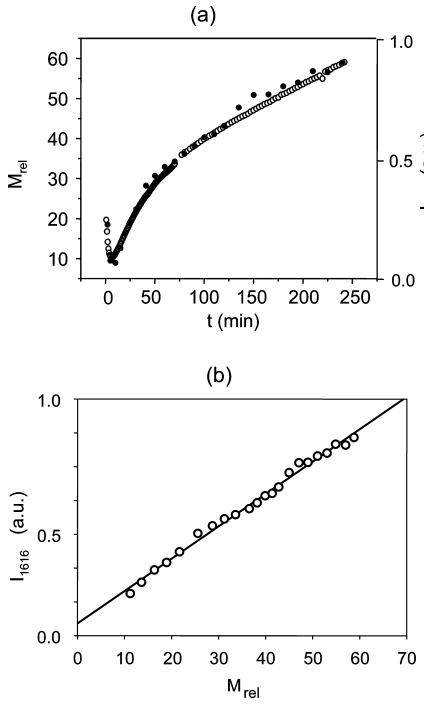

FIGURE 8: Comparison of structural changes accompanying the heat-induced disaggregation/reassociation of β_2m in the presence of 0.2 M NaCl, pH 2.1, at a protein concentration of 1.2 mg/mL. (a) Comparison of the changes in intensity of the IR band at 1616 cm^{-1} (filled circles) with the changes in aggregate size (open circles). (b) Temporal changes of the IR band at 1616 cm^{-1} versus changes of the relative molecular mass, observed over a time period of 4 h.

the change in IR signal and the mass increase over the entire time range of reassociation was observed (Figure 8b). Thus, the observed temperature-induced behavior of the two structural probes was clearly different from that of the salt-induced changes described before (see Figure 3b). Altogether, the observed heat-induced structural changes suggested a conversion of the salt-induced β_2m "A-type" particles into a different species (here termed "B-type" structures). To evaluate changes in tertiary structure, we have also measured near-UV CD spectra of different conformational states of β_2m (Figure S2 of the Supporting Information). These spectra indicated that subtle changes in the tertiary structure take place during formation of the "A-type" particles. More drastic spectral changes were observed during mild heat treatment of the "A-type" assemblies. A lack of signal in the near-UV range was observed within 10−15 min after the T-jump to 50 °C, similar to the spectrum of acid-unfolded β_2m and suggesting that the tertiary structure of the "A-type" particles could easily disaggregated. Later reassembly into much larger structures was associated with major changes in the near-UV CD spectra. The spectrum obtained after 20 h at 50 °C exhibited a strong negative ellipticity at 280 nm, quite different from spectra of the salt-induced "A-type" assemblies, demonstrating that the tertiary structures of the "A-type" and "B-type" species must be different. The EM micrographs of the heat-treated assemblies revealed the dominance of thin filaments (~6 nm in width) with an average length of ~80 nm (Figure 4b,d). Keeping the samples containing the filaments for up to 11 months at room temperature led to a further increase of the average length of the filaments, also called protofibrils by others (*21*). However, amyloid-like structures characterized by intertwined filaments were not observed in any of the EM micrographs of the corresponding samples (Figure S3 of the Supporting Information).

Heat-Triggered Conversion of the "A-Type" Particles into Amyloid Fibrils. During our search for conditions which could promote the formation of fibrils, we explored the effect of extended heat treatment on the salt-induced assemblies of β_2m using infrared spectroscopy. The spectra of the "A-type" particles obtained at discrete temperatures by heating the samples from 20 to 100 °C in steps of 5 °C revealed clear-cut spectral changes, and the spectrum of the sample after cooling from 100 to 25 °C was quite different from the one obtained before heating (compare the dashed and solid traces in Figure 9a,b). Its major amide I band component appeared around 1618 cm^{-1} compared to 1615 cm^{-1} in the initial state. Most strikingly, however, the high-frequency β-sheet component at 1685 cm^{-1} was not evident from the spectrum after heat treatment, indicating that the intermolecular β-sheet structure of the new state was different from that of the "A-type" structure. This suggested a parallel organization of the strands in the new aggregation state of β_2m, because the high-frequency β-component arises specifically from an antiparallel β-sheet structure (*35, 36*). Moreover, the heat-triggered conversion of the β_2m structure was also associated with changes in the microenvironment of the tyrosine side chains, indicated by the different peak positions of the tyrosine band for the two states (Figure 9b,c). Since the shape of the corresponding tyrosine bands was not affected, the 1.0 cm^{-1} difference in frequency at 25 °C (1515.3 cm^{-1} in the "A-type" vs 1516.3 cm^{-1} in the fibrils) most likely reflected differences in the microenvironment of all tyrosine residues of β_2m. The intensity/temperature (Figure 9c, triangles) and frequency/temperature (Figure 9c, circles) profiles for the IR band at 1685 cm^{-1} and the tyrosine band, respectively, indicated sigmoidal spectral changes between 55 and 85 °C, with midpoint transition temperatures of ~66 °C.

The spectra of the "B-type" particles revealed only minor changes between 20 and 90 °C, and the spectrum obtained after cooling from 90 to 25 °C was almost identical to that obtained at 25 °C before heating (Figure S4 of the Supporting Information). This proved that the structure of the "B-type" species obtained after mild heat treatment of the "A-type" form was much more stable than that of the initial short assemblies and not amenable to further structural changes.

Amyloid Fibrils Formed at Low pH by Agitation. Finally, we also obtained IR spectra of fibrils of β_2m formed at low ionic strength by agitating the protein solution. For technical reasons, this was not feasible directly in the IR cell. As an alternative, the acid-unfolded β_2m molecules in 0.05 M NaCl (pH 2.1) were agitated by the magnetic stirrer in a fluorescence cell of the spectrofluorometer for 24 h at 37 °C. The agitation resulted in association of the molecules, which was monitored by light scattering measurements at 500 nm (data not shown), and at certain times after initiation of the reaction aliquots of 15 μL were taken for analysis by IR spectroscopy. The spectrum of an aliquot taken after 70 min was characterized by a nearly featureless amide I band contour centered at 1639 cm^{-1} (Figure 9d, dotted trace), practically identical to the spectrum of β_2m in 2 mM DCl (Figure 2b), suggesting that no secondary structure was formed within the first hour. Conspicuous spectral features, however, were observed after

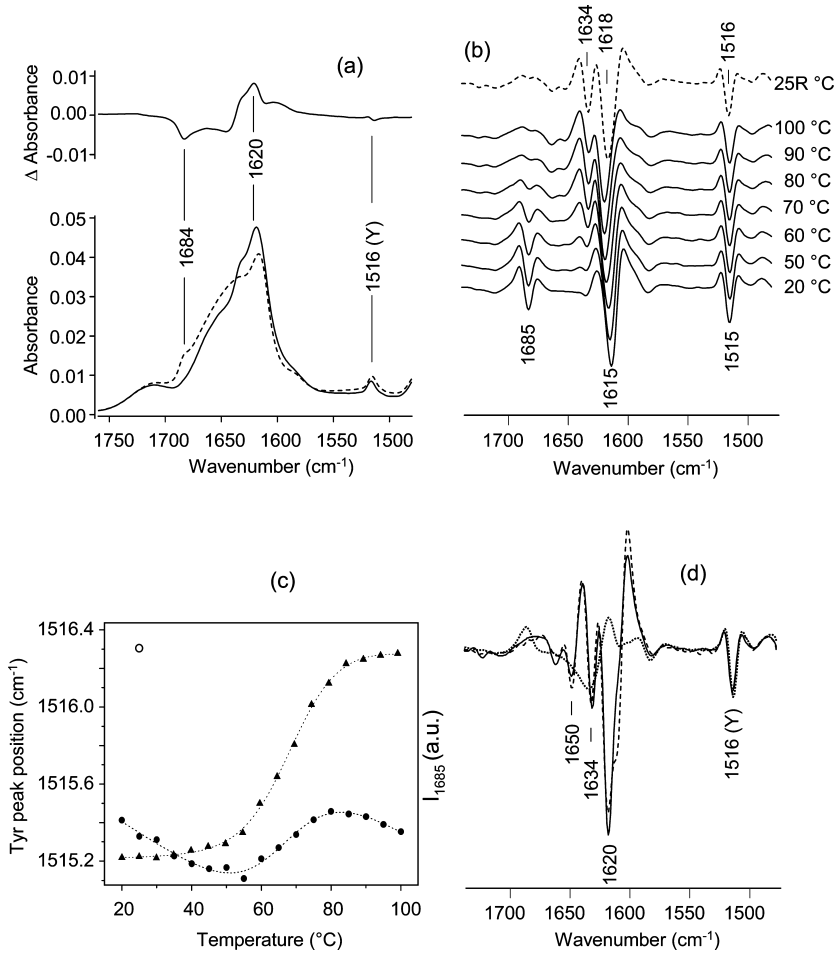

FIGURE 9: IR spectroscopy data of different forms of β_2m aggregates. (a) IR absorbance spectra of salt-induced "A-type" structures (after 2 days at 37 °C, protein concentration 3.2 mg/mL, 0.2 M NaCl, pH 2.1) at 25 °C before heating (dashed line) and after cooling from 100 to 25 °C (solid line). The upper trace shows the corresponding IR difference spectrum (after heating minus before heating). (b) Stacked representation of the second derivatives of the IR spectra of salt-induced "A-type" structures at the indicated temperatures upon heating and after cooling from 100 to 25 °C (25R). (c) Temperature dependence of the position of the tyrosine band (filled circles) and the intensity of the amide I band at 1685 cm^{-1} (filled triangles), respectively, of the "A-type" sample between 20 and 100 °C. The dashed lines represent fits to estimate the corresponding midpoint transition temperatures. The single open circle indicates the position of the tyrosine band after heating to 100 °C and cooling to 25 °C. (d) Second derivatives of the IR spectra agitation-treated β_2m in the presence of 0.05 M NaCl (protein concentration 3.2 mg/mL, pH 2.1, 37 °C) at 70 min (dotted line) and 1 day (dashed line) after initiation of the process in the fluorescence cell. The solid line corresponds to a 3 day sample after heating to 95 °C and cooling to 25 °C in the infrared cell.

1 day, since the spectrum was now dominated by a major amide I band component centered at 1620 cm^{-1} (Figure 9d, dashed trace). The shape of the spectral feature around 1620 cm^{-1} suggested that it was not a single component, but rather a sum of similar spectral components. Altogether, these spectral changes indicated an agitation-induced formation of intermolecular β-sheet structure in the sample after a pronounced lag phase, suggesting a nucleation-induced association mechanism of the β_2m molecules.

Only minor spectral changes were observed after further heating of the sample in the IR cell to 95 °C and cooling to 25 °C. A sharper major infrared band at 1620 cm^{-1} was notable (compare the dashed and solid traces in Figure 9d), suggesting a more uniform intermolecular β-sheet structure after heating. The major infrared spectral features of the latter sample were almost identical to those of "A-type" β_2m species formed after heat treatment to 100 °C (compare dashed trace in Figure 9b and solid trace in Figure 9d), indicating a very similar type of intermolecular β-sheet structure in the two samples. The EM images of these assemblies revealed the presence of long intertwined fibrillar structures (Figure 10a,b) that are characteristic for β_2m amyloid fibrils. The weak feature at 1634 cm^{-1} in the spectra of the two β_2m fibrils (Figure 9b,d), whose position coincided with the dominant band observed for β_2m in the native fold (Figure 2a), could indicate backbone C═O groups involved in some intramolecular β-sheet structure in the amyloid samples. However, the assignment of this band, which did not change after the agitation-induced fibrils were heated to 95 °C and then cooled to 25 °C, remains uncertain. This was also true for the weak feature at 1650 cm^{-1} in the spectrum of the fibrils (Figure 9d), since it was unlikely that it could have arisen from α-helices or loops, such as typically observed in the IR spectra of globular proteins (*36*). Possibly, the band components at 1634 and 1650 cm^{-1} reflect a characteristic arrangement of β-strands in the fibrils, which cannot be specified based on currently known structure−spectrum correlations.

DISCUSSION

The conversion of individual β_2m molecules into large assemblies involves changes in structure as well as in the association state. To monitor these changes, we conducted

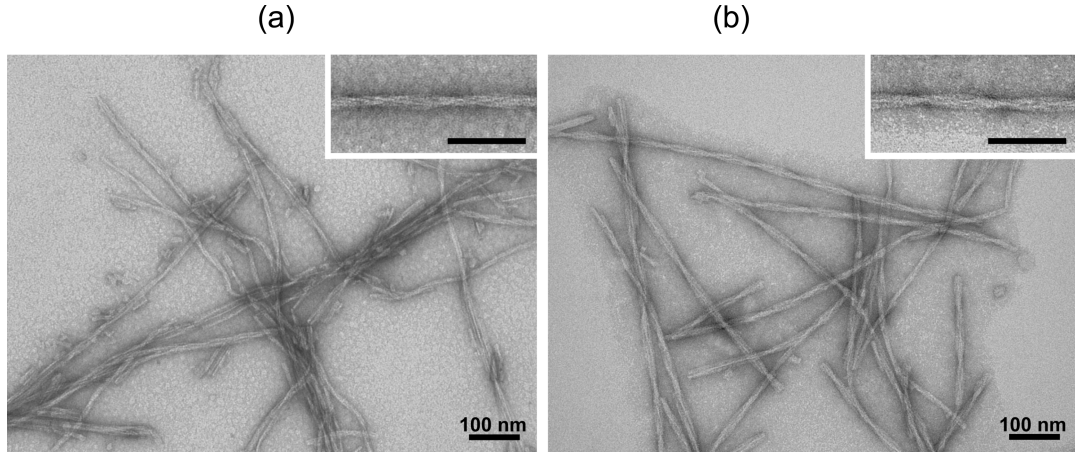

FIGURE 10: Electron micrographs of β_2m amyloid fibrils. (a) Fibrils obtained after heating of the "A-type" assemblies in the presence of 0.2 M NaCl at pH 2.1 to 100 °C. (b) Agitation-induced fibrils of β_2m obtained at 37 °C in the presence of 0.05 M NaCl at pH 2.1. The insets in (a) and (b) show enlarged views of single fibrils (scale bars, 100 nm).

a series of experiments to identify and characterize products emerging during assembly. Changes in the oligomeric state of β_2m were probed by light scattering techniques (SLS and DLS), while changes of its secondary structure were assessed directly by IR spectroscopy. Light scattering experiments can be performed at the same experimental conditions (medium to high protein concentrations, D_2O as solvent) as applied for IR studies. Therefore, we combined both experimental approaches (*37–39*) in order to correlate changes in secondary and tertiary structure of β_2m with its state of oligomerization.

Consistent with previous reports (*40*), acid-unfolded β_2m at pH 2.4 was found to be monomeric with an increased Stokes radius, when compared to natively folded β_2m. The addition of sodium chloride led to association of the molecules and to the generation of short curved structures, here termed "A-type" particles, that have also been observed by other authors (*16, 17, 22*). Changes in integrated light scattering intensity were observed immediately after addition of salt, suggesting that the aggregation process was not dominated by a nucleation barrier, while SLS/DLS data indicated that dimeric to tetrameric species were formed within the first 2 min upon initiation of association. Parallel IR experiments indicated the presence of β-strands organized in an antiparallel intramolecular-like fashion shortly after addition of NaCl to the acid-denatured β_2m solution. NMR data had shown that β_2m at pH 3.4−3.6 is a partially unfolded molecule (*16, 41*), which retains a stable structure in five of the seven β-strands that comprise the native state. Moreover, it has been suggested that the β_2m conformation formed at pH 3.6 represents an amyloid precursor conformation (*41*). The similarity of the IR spectra of the initial salt-induced state of β_2m obtained at pH 2.1 to those measured at pH 3.4 suggests that native-like structural elements must be present in the former state. In addition, the IR data demonstrate that the initial intramolecular-like structure disappears over time, a process which is accompanied by the formation of intermolecular β-sheet structure.

However, the kinetics of this intermolecular β-sheet formation differs from that of β_2m association, revealing two phases (Figure 3b). A linear relation between the formation of β-aggregates and particle growth can only be observed until octamers to decamers are formed, while the formation of larger particles (20-mers) involves only minor changes in secondary structure (Figure 3a). As the secondary structure, the size, and the morphology of these oligomers were stable for months at room temperature, one could consider these "A-type" structures as dead-end products separated from the pathway leading to mature fibrils, in agreement with a previous report (*20*). Limited proteolysis of short curved assemblies of β_2m formed at pH 2.5 had already revealed that these are not tightly organized, with only ~30 residues of the central region of the polypeptide chain being protected from proteolysis (*42*). We could show here that these "A-type" particles can reassemble into much larger particles with an average length of ~80 nm (here termed "B-type" structures) upon mild heat treatment, a process which is accompanied by disruption of the initial intermolecular β-sheet structure and the re-formation of a new one. Moreover, a linear correlation between increasing intermolecular β-sheet structure and mass increase was noticed over the entire time range of observation (Figure 8b), in contrast to the salt-induced changes discussed before (Figure 3b). This indicates different mechanisms for the assembly of the "A-type" and "B-type" filaments. In the former case, small oligomers seem to play a key role during the formation of the short curved particles, since the formation of intermolecular β-sheet structure almost comes to an end at this stage. Such small oligomeric structures, termed critical oligomers, were also observed during misfolding of other proteins, such as the Syrian hamster prion protein (*38*) or yeast phosphoglycerate kinase (*39*). The organization of the polypeptide chain during assembly of the longer "B-type" particles differed considerably from that of the initial salt-induced structures and led to an intermolecular β-sheet structure, which was not amenable to structural changes by thermal heating.

Finally, we were able to convert the "A-type" particles of β_2m into amyloid fibrils by extended heat treatment. Interestingly, among other spectral changes associated with this conversion process, we observed the disappearance of the band at 1684 cm^{-1} and an upshift of the main amide I peak by three wavenumbers from 1615 to 1618 cm^{-1} (Figure 9b). We suggest that the polypeptide conformation must have been rearranged significantly during this conversion event, resulting in long and straight fibrils. Independent support for a significant structural rearrangement comes from the spectral changes of the absorption band of the tyrosine side chain at ~1516 cm^{-1}, which is a sensitive local monitor of protein

conformation (*33, 43, 44*). There are six tyrosine residues in β_2m, of which five residues form a cluster, while one residue is located far apart from this cluster in the natively folded state. The heat-induced shift of the peak position of the tyrosine band by one wavenumber, but without modifying its shape (Figure 9c), indicates that most likely all of the tyrosine residues experience changes in their microenvironment as a consequence of fibril formation. This conversion process could be quite significant and may involve the conversion of β-sheet structures from an antiparallel to a parallel architecture of the intermolecular peptide chains. We take the absence of the spectral component at $\sim$1684 cm^{-1} in the IR spectra of the fibrils (see dashed trace in Figure 9b and solid trace in Figure 9d) as a strong support of this view, as this spectral feature is essentially absent in the spectra of mature fibrils of β_2m prepared by seed-dependent polymerization at pH 2.5 (*15*), and in the IR spectra of mature fibrils of other proteins, such as insulin (*45*), the SH3 domain (*46, 47*), lysozyme (*48*), or peptide models (*49*). At the same time, these reports have shown that the high-frequency component at $\sim$1684 cm^{-1} is well expressed by amorphous aggregates (*45, 46*) or curved worm-like filaments (*49*).

Theoretical calculations have suggested that it is possible to distinguish antiparallel β-sheet structures from their parallel counterparts by IR spectroscopy, since the latter lack the high-frequency component (*35*). Moreover, the strong low-frequency amide I band component of an antiparallel β-sheet is expected to absorb at slightly lower frequency when compared to that of a parallel β-sheet. These theoretical suggestions are supported by experimental studies on model peptides (*50, 51*). The different assemblies of β_2m produced here reveal just these spectral features, i.e., a major band component at $\sim$1616 cm^{-1} and a weaker band component at $\sim$1684 cm^{-1} for the short curved structures, but only a strong low-frequency band component at $\sim$1618/20 cm^{-1} for the long and straight fibrils (Figure 9b,d), suggesting a parallel organization of the strands in the fibrils of β_2m in the latter case, which is in agreement with IR studies of mature fibrils of β_2m prepared by seed-dependent polymerization at pH 2.5 (*15*).

A strong band component at $\sim$1624 cm^{-1}, but no spectral feature around 1684 cm^{-1}, was also observed in the IR spectra of fibrils of the so-called K3 fragment (Ser20−Lys41) of β_2m (*52*). The conformation of K3 fibrils was found to consist of a β-strand−loop−β-strand with each K3 molecule stacked in a parallel and staggered manner, based on solid-state NMR data (*53*). Altogether, these largely empirical correlations strongly support the assumption that the β-sheet structures in β_2m fibrils obtained here at acidic pH consist largely of parallel β-strands. However, since variations in hydrogen-bonding strength as well as differences in transition dipole coupling in distinct β-strands can influence the positions of the characteristic β-sheet bands, the specific geometry of β-strands in the fibrils could perturb the frequencies in a manner distinguishable from those in native β-sheet structures. Theoretical studies have indicated that the number of strands in a β-sheet and local conformational disorder impact on the spectral features in the amide I region (*54–56*). Apart from remaining uncertainties in correlating IR spectral features with three-dimensional structural details, the present work illustrates that the IR technique is a very sensitive approach to characterize different β-structures and to probe conformational changes within them. Moreover, IR spectroscopy is not vulnerable to light scattering artifacts, such as CD spectroscopy, and is, thus, particularly useful in studying aggregation processes of β_2m that may be important in dialysis-related amyloidosis.

ACKNOWLEDGMENT

We are grateful to Dr. Hans Huser for help with the β_2m preparations and the anonymous reviewers for constructive criticism.

SUPPORTING INFORMATION AVAILABLE

A figure showing the initial salt-induced relative mass increase of β_2m at three protein concentrations as monitored by DLS, a figure comparing near-UV CD spectra of different conformational states of β_2m (native, acid-denatured, salt-induced "A-type" particles, heat-induced "B-type" structures), a figure showing an EM micrograph of the "B-type" particles after 11 months at room temperatures, and a figure showing temperature-induced changes in the IR spectra of the "B-type" particles. This material is available free of charge via the Internet at http://pubs.acs.org.

REFERENCES

1. Bjorkman, P. J., Saper, M. A., Samraoui, B., Bennett, W. S., Strominger, J. L., and Wiley, D. C. (1987) Structure of the human class I histocompatibility antigen, HLA-A2. *Nature 329*, 506–512.
2. Saper, M. A., Bjorkman, P. J., and Wiley, D. C. (1991) Refined structure of the human histocompatibility antigen HLA-A2 at 2.6 Å resolution. *J. Mol. Biol. 219*, 277–319.
3. Gejyo, F., Yamada, T., Odani, S., Nakagawa, Y., Arakawa, M., Kunitomo, T., Kataoka, H., Suzuki, M., Hirasawa, Y., Shirahama, T., Cohen, A. S., and Schmid, K. (1985) A new form of amyloid protein associated with chronic hemodialysis was identified as β_2-microglobulin. *Biochem. Biophys. Res. Commun. 129*, 701–706.
4. Gorevic, P. D., Casey, T. T., Stone, W. J., Diraimondo, C. R., Prelli, F. C., and Frangione, B. (1985) β_2-microglobulin is an amyloidogenic protein in man. *J. Clin. Invest. 76*, 2425–2429.
5. Floege, J., and Ketteler, M. (2001) β_2-microglobulin-derived amyloidosis: an update. *Kidney Int. 59*, S164–S171.
6. Morgan, C. J., Gelfand, M., Atreya, C., and Miranker, A. D. (2001) Kidney dialysis-associated amyloidosis: a molecular role for copper in fiber formation. *J. Mol. Biol. 309*, 339–345.
7. Eakin, C. M., Attenello, F. J., Morgan, C. J., and Miranker, A. D. (2004) Oligomeric assembly of native-like precursors precedes amyloid formation by β_2-microglobulin. *Biochemistry 43*, 7808–7815.
8. Esposito, G., Michelutti, R., Verdone, G., Viglino, P., Hernandez, H., Robinson, C. V., Amoresano, A., Dal Piaz, F., Monti, M., Pucci, P., Mangione, P., Stoppini, M., Merlini, G., Ferri, G., and Belotti, V. (2000) Removal of the N-terminal hexapeptide from human β_2-microglobulin facilitates protein aggregation and fibril formation. *Protein Sci. 9*, 831–845.
9. Yamamoto, S., Yamaguchi, I., Hasegawa, K., Tsutsumi, S., Goto, Y., Gejyo, F., and Naiki, H. (2004) Glycosaminoglycans enhance the trifluoroethanol-induced extension of β_2-microglobulin-related amyloid fibrils at a neutral pH. *J. Am. Soc. Nephrol. 15*, 126–133.
10. Yamamoto, S., Hasegawa, K., Yamaguchi, I., Tsutsumi, S., Kardos, J., Goto, Y., Gejyo, F., and Naiki, H. (2004) Low concentrations of sodium dodecyl sulfate induce the extension of β_2-microglobulin-related amyloid fibrils at neutral pH. *Biochemistry 43*, 11075–11082.
11. Ohhashi, Y., Kihara, M., Naiki, H., and Goto, Y. (2005) Ultrasonication-induced amyloid fibril formation of β_2-microglobulin. *J. Biol. Chem. 280*, 32843–32848.
12. Kihara, M., Catani, E., Sakai, K., Hasegawa, K., Naiki, H., and Goto, Y. (2005) Seeding-dependent maturation of β_2-microglobulin amyloid fibrils at neutral pH. *J. Biol. Chem. 280*, 12012–12018.

13. Relini, A., Canale, C., DeStefano, S., Rolandi, R., Giorgetti, S., Stoppini, M., Rossi, A., Fogolari, F., Corazza, A., Esposito, G., Gliozzi, A., and Belotti, V. (2006) Collagen plays an active role in the aggregation of β_2-microglobulin under physiopathlogical conditions of dialysis-related amyloidosis. *J. Biol. Chem. 281*, 16521–16529.
14. Naiki, H., Hasimoto, N., Suzuki, S., Kimura, H., Nakakuki, K., and Gejyo, F. (1997) Establishment of a kinetic model of dialysis-related amyloid fibril extension in vitro. *Amyloid 4*, 223–232.
15. Kardos, J., Okuno, D., Kawai, T., Hagihara, Y., Yumoto, N., Kitagawa, T., Zavodszky, P., Naiki, H., and Goto, Y. (2005) Structural studies reveal that the diverse morphology of β_2-microglobulin aggregates is a reflection of different molecular architectures. *Biochim. Biophys. Acta 1753*, 108–120.
16. McParland, V. J., Kad, N. M., Kalverda, A. P., Brown, A., Kirwin-Jones, P., Hunter, M. G., Sunde, M., and Radford, S. E. (2000) Partially unfolded states of β_2-microglobulin and amyloid formation *in vitro*. *Biochemistry 39*, 8735–8746.
17. Kad, N. M., Myers, S. L., Smith, D. P., Smith, D. A., Radford, S. E., and Thomson, N. H. (2003) Hierarchical assembly of β_2-microglobulin amyloid *in vitro* revealed by atomic force microscopy. *J. Mol. Biol. 330*, 785–797.
18. Smith, D. P., Jones, S., Serpell, L. C., Sunde, M., and Radford, S. E. (2003) A systematic investigation into the effect of protein destabilization on β_2-microglobulin amyloid formation. *J. Mol. Biol. 330*, 943–954.
19. Radford, S. E., Gosal, W. S., and Platt, G. W. (2005) Towards an understanding of the structural molecular mechanism of β_2-microglobulin amyloid formation in vitro. *Biochim. Biophys. Acta 1753*, 51–63.
20. Gosal, W. S., Morten, I. J., Hewitt, E. W., Smith, D. A., Thomson, N. H., and Radford, S. E. (2005) Competing pathways determine fibril morphology in the self-assembly of β_2-microglobulin into amyloid. *J. Mol. Biol. 351*, 850–864.
21. Smith, A. M., Jahn, T. R., Ashcroft, A. E., and Radford, S. E. (2006) Direct observation of oligomeric species formed in the early stages of amyloid fibril formation using electrospray ionization mass spectrometry. *J. Mol. Biol. 364*, 9–19.
22. Hong, D.-P., Gozu, M., Hasegawa, K., Naiki, H., and Goto, Y. (2002) Conformation of β_2-microglobulin amyloid fibrils analyzed by reduction of the disulfide bond. *J. Biol. Chem. 277*, 21554–21560.
23. Sasahara, K., Yagi, H., Naiki, H., and Goto, Y. (2007) Heat-triggered conversion of protofibrils into mature amyloid fibrils of β_2-microglobulin. *Biochemistry 46*, 3286–3293.
24. Myers, S. L., Jones, S., Jahn, T. R., Morten, I. J., Tennent, G. A., Hewitt, E. W., and Radford, S. E. (2006) A systematic study of the effect of physiological factors on β_2-microglobulin amyloid formation at neutral pH. *Biochemistry 45*, 2311–2321.
25. Hülsmeyer, M., Hillig, R. C., Volz, A., Rühl, M., Schröder, W., Saenger, W., Ziegler, A., and Uchanska-Ziegler, B. (2002) HLA-B27 subtypes differentially associated with disease exhibit structural alterations. *J. Biol. Chem. 279*, 47844–47852.
26. Gast, K., Nöppert, A., Müller-Frohne, M., Zirwer, D., and Damaschun, G. (1997) Stopped-flow dynamic light scattering as a method to monitor compaction during protein folding. *Eur. Biophys. J. 25*, 211–219.
27. Provencher, S. W. (1982) Contin—a general-purpose constrained regularization program for inverting noisy linear algebraic and integral equations. *Comput. Phys. Commun. 27*, 229–242.
28. Koppel, D. E. (1972) Analysis of macromolecular polydispersity in intensity correlation spectroscopy: the method of cumulants. *J. Chem. Phys. 57*, 4814–4820.
29. Fabian, H., and Mäntele, W. (2002) *Handbook of Vibrational Spectroscopy, Infrared Spectroscopy of Proteins* (Chalmers, J. M., and Griffiths, P. R., Eds.) pp 3399−3425, Wiley, Chichster, U.K.
30. Rasband, W. S. (1997−2007)ImageJ, National Institutes of Health, Bethesda, MD (http://rsb.info.nih.gov/ij/).
31. Uversky, V. N. (1993) Use of fast protein size-exclusion liquid chromatography to study the unfolding of proteins which denature through the molten globule. *Biochemistry 32*, 13288–13298.
32. Barth, A. (2000) The infrared absorption of amino acid side chains. *Prog. Biophys. Mol. Biol. 74*, 141–173.
33. Fabian, H., Schultz, C., Backmann, J., Hahn, U., Saenger, W., Mantsch, H. H., and Naumann, D. (1994) Impact of point mutations on the structure and thermal stability of ribonuclease T1 in aqueous solution probed by Fourier transform infrared spectroscopy. *Biochemistry 33*, 10725–10730.
34. Gast, K., Modler, A. J., Damaschun, H., Kröber, R., Lutsch, G., Zirwer, D., Golbik, R., and Damaschun, G. (2003) Effect of environmental conditions on aggregation and fibril formation of barstar. *Eur. Biophys. J. 32*, 710–723.
35. Krimm, S., and Bandekar, J. (1996) Vibrational spectroscopy and conformation of peptides, polypeptides and proteins. *Adv. Protein Chem. 38*, 181–364.
36. Arrondo, J. L. R., Muga, A., Castresana, F. M., and Goni, F. M. (1993) Quantitative studies of the structure of proteins in solution by Fourier-transform infrared spectroscopy. *Prog. Biophys. Mol. Biol. 59*, 23–56.
37. Fabian, H., Fälber, K., Gast, K., Reinstädler, D., Rogov, V. V., Naumann, D., Zamyatkin, D. F., and Filimonov, V. V. (1999) Secondary structure and oligomerization behaviour of equilibrium unfolding intermediates of the λ-cro repressor. *Biochemistry 38*, 5633–5642.
38. Sokolowski, F., Modler, A. J., Masuch, R., Zirwer, D., Baier, M., Lutsch, G., Moss, D. A., Gast, K., and Naumann, D. (2003) Formation of critical oligomers is a key event during conformational transition of recombinant syrian hamster prion protein. *J. Biol. Chem. 278*, 40481–40492.
39. Modler, A. J., Fabian, H., Sokolowski, F., Lutsch, G., Gast, K., and Damaschun, G. (2004) Polymerization of proteins into amyloid protofibrils shares common critical oligomeric states but differs in the mechanisms of their formation. *Amyloid 11*, 215–231.
40. Platt, G. W., McParland, V. J., Kalverda, A. P., Homans, S. W., and Radford, S. E. (2005) Dynamics in the unfolded state of β_2-microglobulin studied by NMR. *J. Mol. Biol. 346*, 279–292.
41. McParland, V. J., Kalverda, A. P., Homans, S. W., and Radford, S. E. (2002) Structural properties of an amyloid precursor of β_2-microglobulin. *Nat. Struct. Biol. 9*, 326–331.
42. Myers, S. L., Thomson, N. N., Radford, S. E., and Ashcroft, A. E. (2006) Investigating the structural properties of amyloid-like fibrils formed in vitro from β_2-microglobulin using limited proteolysis and electrotrospray ionisation mass spectrometry. *Rapid Commun. Mass Spectrom. 20*, 1628–1636.
43. Fabian, H., Huser, H., Narzi, D., Misselwitz, R., Loll, B., Ziegler, A., Böckmann, R. A., Uchanska-Ziegler, B., and Naumann, D. (2008) HLA-B27 subtypes differentially associated with disease exhibit conformational differences in solution. *J. Mol. Biol. 376*, 798–810.
44. Tremmel, S., Beyermann, M., Oschkinat, H., Bienert, M., Naumann, D., and Fabian, H. (2005) ^{13}C-labeled tyrosine residues as local IR probes for monitoring conformational changes in peptides and proteins. *Angew. Chem., Int. Ed. 44*, 4631–4635.
45. Bouchard, M., Zurdo, J., Nettleton, E. I., Dobson, C. M., and Robinson, C. V. (2000) Formation of insulin amyloid fibrils followed by FTIR simultaneously with CD and electron microscopy. *Protein Sci. 9*, 1960–1967.
46. Zurdo, J., Guijarro, J. I., Jiminez, J. L., Saibil, H. R., and Dobson, C. M. (2001) Dependence on solution conditions of aggregation and amyloid formation by an SH3 domain. *J. Mol. Biol. 311*, 325–340.
47. Zurdo, J., Guijarro, J. I., and Dobson, C. M. (2001) Preparation and characterization of purified amyloid fibrils. *J. Am. Chem. Soc. 123*, 8141–8142.
48. Frare, E., Mossuto, M. F., Polverino de Laureto, P., Dumoulin, M., Dobson, C. M., and Fontana, A. (2006) Identification of the core structure of lysozyme amyloid fibrils by proteolysis. *J. Mol. Biol. 361*, 551–561.
49. Janek, K., Behlke, J., Zipper, J., Fabian, H., Georgalis, Y., Beyermann, M., Bienert, M., and Krause, E. (1999) Water-soluble β-sheet models which self-assemble into fibrillar structures. *Biochemistry 38*, 8246–8252.
50. Yamada, N., Ariga, K., Naito, M., Matsubara, K., and Koyama, E. (1998) Regulation of β-sheet structures within amyloid-like β-sheet assemblage from tripeptide derivatives. *J. Am. Chem. Soc. 120*, 12192–12199.
51. Chitnumsub, P., Fiori, W. R., Lashuel, H. A., Diaz, H., and Kelly, J. W. (1999) The nucleation of monomeric parallel β-sheet-like structures and their self-assembly in aqueous solution. *Bioorg. Med. Chem. 7*, 39–59.
52. Yamaguchi, K., Takahashi, S., Kawai, T., Naiki, H., and Goto, Y. (2005) Seeding-dependent propagation and maturation of amyloid fibril formation. *J. Mol. Biol. 352*, 952–960.
53. Iwata, K., Fujiwara, T., Matsuki, Y., Akutsu, H., Takahashi, S., Naiki, H., and Goto, Y. (2006) 3D structure of amyloid protofilaments of β_2-microglobulin fragment probed by solid-state NMR. *Proc. Natl. Acad. Sci. U.S.A. 103*, 18119–18124.

54. Kubelka, J., and Keiderling, T. A. (2001) Differentiation of β-sheet-forming structures: Ab initio-based simulations of IR absorption and vibrational CD for model peptide and protein β-sheets. *J. Am. Chem. Soc. 123*, 12048–12058.
55. Demirdöven, N., Cheatum, C. M., Chung, H. S., Khalil, M., and Tokmakoff, A. (2004) Two-dimensional infrared spectroscopy of antiparallel β-sheet secondary structure. *J. Am. Chem. Soc. 126*, 7981–7990.
56. Brauner, J. W., Flach, C. R., and Mendelsohn, R. (2005) A quantitative reconstitution of the amide I contour in the IR spectra of globular proteins: From structure to spectrum. *J. Am. Chem. Soc. 127*, 100–109.

BI800279Y